Paper

Wavelet Analysis of Voltage Disturbances for Power Quality Applications

Non-member	Effrina Yanti Hamid	(Osaka University)
Member	Zen-Ichiro Kawasaki	(Osaka University)
Member	Hirotaka Yoshida	(Kansai Electric Power Co.)
Member	Hirosuke Doi	(Kansai Electric Instrument Co.)

This paper addresses the subject of stationary and non-stationary voltage disturbance problems in electric power system. The modified binary-tree wavelet decomposition technique with an appropriate wavelet filter is introduced as a powerful tool for detecting, classifying, and quantifying the voltage disturbances. Power quality (PQ) indices in terms of total rms, rms of individual frequency bands, duration of disturbance, and their dependent quantities such as voltage magnitude of disturbance and harmonic distortion can be measured directly from the wavelet transform coefficients. The proposed technique is simple, provides accurate value of PQ indices, and enables to discriminate among the type of similar voltage disturbance events. The proposed technique is validated by its application to various disturbance data and the measurement results, such as rms and harmonic distortion, are further compared with those obtained from the time domain and frequency domain methods.

Keywords: Power Quality, Binary-Tree Wavelet Transforms, Voltage Disturbances, Harmonics.

1. Introduction

The quality of electric power has become an important issue for electric utilities and their customers. The quality of electric power is largely synonymous with the voltage quality. Poor voltage quality due to disturbances may cause malfunction of devices, misoperation of sensitive loads, interrupted production processes, and shortened equipment life [1]~[4]. The general strategy to assure voltage quality is to monitor the supply voltage and take appropriate countermeasures based on detection of voltage disturbances which exceed the load tolerance limits [5].

Voltage quality analysis have usually been divided into those which address (1) stationary waveforms, such as harmonics, flat-top, and notching, (2) non-stationary waveforms, such as voltage sag, voltage swell, and momentary interruption, and (3) transient waveforms, like those resulting from faults or capacitor switchings [1] [2] [4] [6]~[8]. Harmonic disturbance occurs most frequently in power system and it does appear in any other disturbances [4]. Hence, for a power quality (PQ) monitoring tool to become widely accepted in power system engineering, it is important that it enables analysis of harmonics [9].

Techniques to visually monitor voltage disturbances have implemented the continuous wavelet transform (CWT) [7] [10], the conventional discrete wavelet transform (DWT) [1] [2] [6], and the combination of them [3] with a specific wavelet filter used. However, most of the works using these techniques deal with detection of disturbances [1] [3] [6] [7], and some include the classification purposes [2] [4] [10], but none is intended to include the quantification purposes. Moreover, CWT techniques are criticized due to their computational redundancy and they are often difficult to be implemented in real-time system. DWT techniques are not suitable for harmonic analysis, because the resulted frequency bands do not have the same width and the results do not give easy insight in the time behavior of the harmonics [9]. In addition, the choice of which wavelet to use in PQ monitoring system also plays an important role [11], because the wavelet affects the accuracy of PQ indices, such as rms, harmonic distortion, and voltage magnitude of disturbances.

A technique to detect, classify, and quantify voltage disturbances is proposed. The technique is based on binary-tree wavelet transform which has been modified to fit the monitoring requirements, and an appropriate wavelet filter has been chosen to yield good quantification. As compared with the recent PQ monitoring system as illustrated in reference [2] and in reference [10] which used respectively the DWT and the CWT, the proposed technique (1) enables harmonic analysis, (2) provides more easy measurement and accurate value of PQ indices, and (3) can be used mainly for both stationary and non-stationary disturbances, besides the ability to discriminate among the type of similar disturbance events.

This paper starts with a brief introduction to binary-tree wavelet theory and it is followed by the rms measurement in wavelet domain. The calculation of magnitude of disturbance and harmonic distortion indices is also presented. The proposed technique is evaluated to several voltage disturbance data with stationary (harmonics and flat-top) and non-stationary (sag, swell, and

momentary interruption) waveforms. The results, such as total rms, rms of individual frequency bands, and harmonic distortion are further compared with those obtained from the time domain and frequency domain (FFT) methods. Although the time domain and frequency domain methods are not suitable to simultaneously detect, classify, and quantify the disturbances, the time domain method is the most accurate and efficient when total rms is concerned, and the frequency domain method permits to measure the rms of individual frequency components and the harmonic distortion index.

2. Binary-Tree Wavelet Transform

2.1 Theory Binary-tree wavelet transform, often called wavelet packet transform, is a generalization of the commonly used conventional DWT. Let $\phi(t)$ and $\psi(t)$ be the scaling function and the corresponding mother wavelet function in the conventional DWT, and define the wavelet functions $\psi^0(t) = \phi(t)$ and $\psi^1(t) = \psi(t)$. Using the well-known "two-scale equations," we can construct the wavelet basis as follows

$$\psi_{j,k}^{2i}(t) = \frac{1}{\sqrt{2^j}}\psi^{2i}\left(\frac{2^j k - t}{2^j}\right) = \sum_n h(n)\psi_{j-1,2k-n}^{i}(t) \quad \cdots (1)$$

$$\psi_{j,k}^{2i+1}(t) = \frac{1}{\sqrt{2^j}}\psi^{2i+1}\left(\frac{2^j k - t}{2^j}\right) = \sum_n g(n)\psi_{j-1,2k-n}^{i}(t), \quad (2)$$

where i is the node number, j is the decomposition level, and$h(n)$ and $g(n)$ are a pair of quadrature mirror filters (QMFs). The wavelet transform coefficients of a given time domain function $f(t)$ at the jth level and kth point are computed via the following recursion relations:

$$d_j^{2i}(k) = \int f(t)\psi_{j,k}^{2i}(t)dt = \sum_n h(n)d_{j-1}^{i}(2k-n) \quad \cdots\cdots (3)$$

$$d_j^{2i+1}(k) = \int f(t)\psi_{j,k}^{2i+1}(t)dt = \sum_n g(n)d_{j-1}^{i}(2k-n). \quad \cdots (4)$$

Later, the function $f(t)$ represents voltage or current waveform.

The orthogonal wavelet transform satisfies the following properties [12]:

$$\int \psi_{j,k}^{p}(t)\psi_{j,k}^{q}(t)dt = 1 \qquad p = q$$

$$\int \psi_{j,k}^{p}(t)\psi_{j,k}^{q}(t)dt = 0 \qquad p \neq q$$

$$\int \psi_{j,k}(t)\psi_{m,k}(t)dt = 0 \qquad j \neq m. \quad \cdots\cdots\cdots\cdots\cdots (5)$$

Binary-tree wavelet decomposition is depicted in Fig. 1. Let the original waveform has 2^N points. The wavelet transform coefficient $d_j^{2i}(k)$ is obtained by convolving the sequence $d_{j-1}^{i}(k)$ with low-pass filter $h(n)$, and then downsampling by a factor of two (3). The coefficient at $d_j^{2i+1}(k)$ is obtained in similar manner but by convolving with high-pass filter $g(n)$. Number of nodes or bands at jth level is 2^j, and every node has 2^{N-j} points or coefficients. The reconstruction for each band has a reversal process which includes upsampling by a factor of two and filtering.

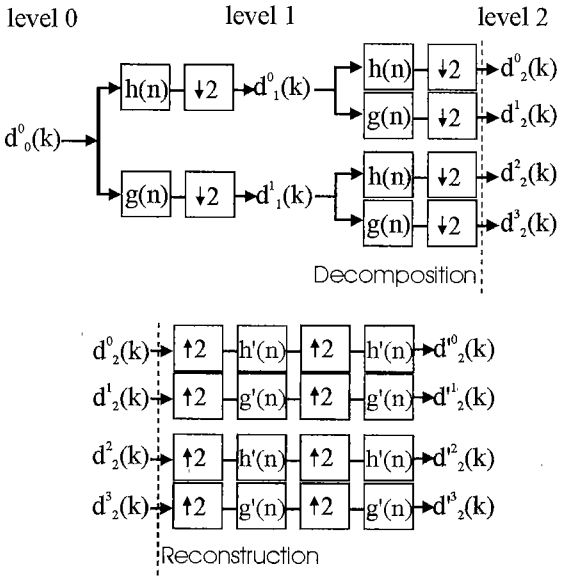

Fig. 1. Binary-tree wavelet decomposition and reconstruction of each band.

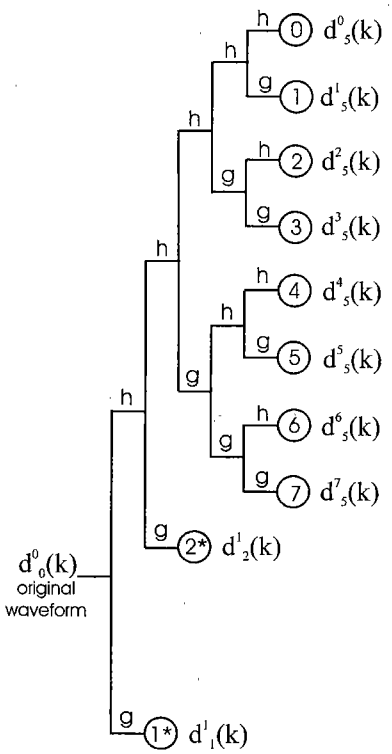

Fig. 2. Modified binary-tree wavelet scheme up to 5th level. Each tree represents the the signal decomposition as illustrated in Fig. 1. The numbers inside each circle indicate the node numbers which are used in the analysis. The h and g represent low-pass and high-pass filters, respectively.

2.2 Modified Binary-Tree Wavelet From a number of analyzed disturbance waveforms, which will be further discussed in the Section 5, we experienced that individual frequency components up to the 15th component are dominant in any disturbance. For this reason we modify the binary-tree wavelet structure to a

more suitable one for monitoring voltage quality. Figure 2 shows the scheme of modified 5-level binary-tree structure. Nodes 0 to 7 have the same frequency bandwidth and are important for harmonic identification purposes. Whereas nodes 1* and 2* have finer resolution levels and are mainly used to detect and localize any disturbance in the signal [2]. Later, in the Section 5, node 0 is the lowest band of the original waveform and includes the fundamental frequency component, nodes 1 to 7 include the waveform of individual band odd harmonics up to 15th component, and nodes 1* to 2* cover the waveforms of successively higher harmonics.

Note that one may easily modify the binary-tree wavelet structure to another scheme if one would treat other individual frequencies of interest which may appear in disturbances other than the disturbances analyzed in this paper. For instance, if one is interested in the frequencies higher than the 15th component, one may expand the node(s) 2* and/or 1* to the higher level of decomposition to produce more children nodes until these nodes cover individual frequencies of interest.

2.3 Choice of Wavelets The choice of wavelets plays an important role in PQ analysis. It depends strongly on particular applications. For detection and localization of short and fast (transient) disturbances, shorter filters (such as Daubechies4 and Daubechies6) are better, while for slow transient disturbances, long filters (such as Daubechies8 and Daubechies10) are particularly good [1] [8] [13]. However, when the accurate measurements/quantifications are concerned, the filters which have good frequency separation are required [11]. Long filters generally have better frequency separation and lower distortion than shorter filters.

The use of Daubechies family filters for detection and localization using a short filter has been exploited in references [1], [3], [4], and [6]. Another filter family, that is Morlet filter, for detection and localization is explained in reference [7]. References [2] and [10] are worth reading to know the application of, respectively, Daubechies and Chaari wavelet filters to both detection and classification. Furthermore, a brief comparison between short and long filters in the same Daubechies family for slow transient and oscillating waveforms can be read in reference [8]. It is worth noting that the previous authors applied a specific filter to a specific application. Meaning that a filter which is good for one purpose most probably it will not be good for other purposes. Therefore, if one is interested to use one type of filter for several purposes (in the present case is for: (1) detection and localization, (2) classification, and (3) quantification), one should select a compromise filter for these purposes. To simplify this formidable task, we employ one type of wavelet filter for whole type of disturbances. The Vaidyanathan filter with 24 coefficients is used in the analysis. This filter is categorized as a long filter, so that it is useful for detecting slow transient disturbances [1] [8] [13] and, because this filter has good frequency separation [12], it is also good for quantification purpose [11]. The coefficients of this filter can be found in reference [12].

3. Power Quality Indices Measurements

To classify the type of disturbances and quantify the PQ indices (such as total rms, rms value of individual frequency bands, harmonic distortion, and voltage magnitude during disturbance), the measurement of rms value with respect to individual bands, the magnitude of disturbance, and the harmonic distortion index is derived.

3.1 RMS Measurement in Wavelet Domain Consider the 5-level binary-tree scheme as depicted in Fig. 2, and let $v(t)$ be the voltage waveform during the observation period T with the total length of 2^N points. In the wavelet theory, any time domain waveform can be expanded as a linear combination of weighted sums of wavelet functions $\psi(t)$ [12] [14]. Hence, the voltage $v(t)$ can be represented in wavelet domain as

$$v(t) = \sum_{i=0}^{7} \sum_{k=0}^{2^{N-5}-1} d_5^i(k)\psi_{5,k}^i(t) + \sum_{j=1}^{2} \sum_{k=0}^{2^{N-j}-1} d_j^1(k)\psi_{j,k}^1(t), \tag{6}$$

where $d_5^i(k), i = 0, 1, ..., 7$, is the wavelet transform coefficients at $j = 5$, and $d_j^1(k)$ is the coefficients at node 1* if $j = 1$ or at node 2* if $j = 2$.

The rms of voltage (V_{rms}) can be derived using (6) based on the wavelet properties in (5) as follows [11]:

$$\begin{aligned}
\int v(t)^2 dt &= \int \left[\sum_{i=0}^{7} \sum_{k=0}^{2^{N-5}-1} d_5^i(k)\psi_{5,k}^i(t) + \sum_{j=1}^{2} \sum_{k=0}^{2^{N-j}-1} d_j^1(k)\psi_{j,k}^1(t) \right]^2 dt \\
&= \int \left[\sum_{i=0}^{7} \sum_{k=0}^{2^{N-5}-1} d_5^i(k)\psi_{5,k}^i(t) \right]^2 dt \\
&+ \int \left[\sum_{j=1}^{2} \sum_{k=0}^{2^{N-j}-1} d_j^1(k)\psi_{j,k}^1(t) \right]^2 dt \\
&+ 2 \int \sum_{i=0}^{7} \sum_{j=1}^{2} \sum_{k=0}^{2^{N-5}-1} d_5^i(k) \sum_{k=0}^{2^{N-j}-1} d_j^1(k)\psi_{5,k}^i(t)\psi_{j,k}^1(t) dt \\
&= \sum_{i=0}^{7} \sum_{k=0}^{2^{N-j}-1} (d_5^i(k))^2 \int (\psi_{5,k}^i(t))^2 dt \\
&+ \sum_{j=1}^{2} \sum_{k=0}^{2^{N-j}-1} (d_j^1(k))^2 \int (\psi_{j,k}^1(t))^2 dt \\
&+ 2 \sum_{i=0}^{7} \sum_{j=1}^{2} \sum_{k=0}^{2^{N-5}-1} d_5^i(k) \sum_{k=0}^{2^{N-j}-1} d_j^1(k) \int \psi_{5,k}^i(t)\psi_{j,k}^1(t) dt,
\end{aligned}$$

from the wavelet properties in (5) it is known that $\int (\psi_{5,k}^i(t))^2 dt = 1$, $\int (\psi_{j,k}^1(t))^2 dt = 1$, and $\int \psi_{5,k}^i(t)\psi_{j,k}^1(t) dt = 0$, therefore, the equation above can be simplified to

$$\int v(t)^2 dt = \sum_{i=0}^{7} \sum_{k=0}^{2^{N-5}-1} (d_5^i(k))^2 + \sum_{j=1}^{2} \sum_{k=0}^{2^{N-j}-1} (d_j^1(k))^2. \tag{7}$$

The (total) rms of $v(t)$ in the time domain, according to IEEE Std. 100-88, is

$$V_{rms} = \sqrt{\frac{1}{T} \int_0^T v(t)^2 dt}, \tag{8}$$

then, by substituting (7) to (8) and $T = 2^N$, the total

rms in the wavelet domain is

$$V_{rms} = \sqrt{\frac{1}{2^N}\left[\sum_{i=0}^{7}\sum_{k=0}^{2^{N-5}-1}(d_5^i(k))^2 + \sum_{j=1}^{2}\sum_{k=0}^{2^{N-j}-1}(d_j^1(k))^2\right]}$$
$$= \sqrt{\sum_{i=0}^{7}(V_5^i)^2 + \sum_{j=1}^{2}(V_j^1)^2}, \quad \cdots\cdots (9)$$

where

$$V_5^i = \sqrt{\frac{1}{2^N}\sum_{k=0}^{2^{N-5}-1}(d_5^i(k))^2}, \quad V_j^1 = \sqrt{\frac{1}{2^N}\sum_{k=0}^{2^{N-j}-1}(d_j^1(k))^2}.$$

Here, V_5^i is the rms value of the band at $j = 5$ and node i, and V_j^1 is the rms value of the band at node 1* if $j = 1$ or at node 2* if $j = 2$.

3.2 **Voltage Magnitude of Disturbance** The essence of non-stationary disturbances, such as sag, swell, and momentary interruption, is the sudden change of magnitude of the fundamental frequency for more than 0.5 cycles [2]. When the absolute minima or maxima falls within 10-90% of its nominal voltage, a sag disturbance is then declared. Swell disturbance occurs when the voltage magnitude increases to more than 10% of its nominal voltage. Momentary interruption is similar to the sag disturbance but occurs when the voltage magnitude is less than 10% of its nominal voltage. Since nominal voltage is particulary related to the fundamental frequency component, the non-stationary disturbances are identified by measuring the voltage rms at the lowest band (node 0). The voltage magnitude (V_m) during the disturbance is quantified using a simple formulation as follows (see Appendix)

$$V_m = \sqrt{\frac{V_0^2 T\omega - \omega(T - T_1) - 0.5\sin 2\omega(T - T_1)}{0.5\omega T_1 + 0.25\sin 2\omega T_1}} \text{ p.u.}, \quad (10)$$

where V_0 is the voltage rms in p.u. at the lowest band (that is V_5^i at $i = 0$), ω is the fundamental angular frequency, and T_1 is the duration of disturbance which is obtained from the localization property at either node 1* or node 2*.

3.3 **Total Harmonic Band Distortion** The harmonic distortion index in term of total harmonic band distortion (THBD) can be calculated directly using wavelet transform coefficients associated with the voltage waveform as written in (9). We put the word 'band' in the THBD because the binary-tree wavelet transform can not extract any single frequency component. Rather, this transform brings a frequency band around the frequency of interest. The THBD is defined as the ratio of the rms value of all frequency (harmonic) bands, except of the lowest band, to the rms value of the original distorted waveform:

$$THBD(\%) = \frac{1}{V_{rms}}\sqrt{\sum_{i=1}^{7}(V_5^i)^2 + \sum_{j=1}^{2}(V_j^1)^2} \times 100. \quad (11)$$

4. Execution of Proposed Technique

4.1 **Detecting and Classifying** Plotting the rms value of the lowest band, one will have the ability to recognize the waveform as stationary or non-stationary (later, this plot corresponds to the distribution panel). In case of non-stationary, it is often difficult to distinguish between sag and momentary interruption by using only the plot. Combining this plot with the voltage magnitude measurement (Eq. 10), this difficulty can be solved. Plotting the rms values of each higher band, particularly nodes 1~7, the harmonics of original waveform can be identified. Furthermore, using the localization property at either node 1* or node 2*, it helps to determine the interval of the non-stationary disturbance and to distinguish between harmonic and flat-top waveforms. Therefore, the localization property at node 1* or node 2* may also be used to classify the disturbance as stationary or non-stationary.

4.2 **Quantifying** Quantifying the PQ indices accurately is an important issue to measure the quality of electric power. In the case of stationary waveforms which include harmonics and flat-top, the quality is indicated by the total rms, the rms of individual bands, and the THBD. However, in the case of non-stationary waveforms, the quality is indicated mainly by the peak or rms of fundamental frequency during the disturbance and the disturbance interval. It is noted that as the magnitude and/or duration of the waveform change(s) during the disturbance, the rms value at the lowest band will also change during the observation period.

5. Evaluation and Results

The proposed technique has been applied to a number of stationary and non-stationary disturbance waveforms. The waveforms were generated from an analog power system simulator (APSA: Advanced Power System Analyzer) owned by The Kansai Electric Power Co., Japan. Each voltage waveform has eight 60 Hz fundamental cycles with the sampling frequency used is 7680 Hz or 128 points per 60 Hz cycle. They are decomposed using the modified binary-tree wavelet transform (BTWT) as shown in Fig. 2. Table 1 shows the node numbers with the associated numbers of coefficients, frequency bands, and the odd harmonics which are included in these frequency bands. The first eight bands are enough to see the individual harmonic behaviors up to the 15th component since the rms value of higher harmonic components is generally very small. The representative disturbances are analyzed and discussed below.

Table 1. Individual bands resulted from BTWT.

Node	# of coeffs.	Band(Hz)	Band Odd Harmonics
0	32	DC - 120	1st
1	32	120 - 240	3rd
2	32	240 - 360	5th
3	32	360 - 480	7th
4	32	480 - 600	9th
5	32	600 - 720	11th
6	32	720 - 840	13th
7	32	840 - 960	15th
2*	256	960 - 1920	17th - 31st
1*	512	1920 - 3840	33rd - 63rd

5.1 **Stationary Disturbances** These disturbances have waveforms which are periodic under steady state condition.

Normal Condition: Although this waveform is not a disturbance, but it will be used as a comparison. The waveform under normal condition is shown in Fig. 3. The top panel shows the original waveform, the horizontal bars at the bottom right panel indicate the distribution of rms with respect to the individual bands (we call this as the 'distribution panel'), and the bottom left panel is the time-frequency panel which displays the reconstructed waveform associated with the wavelet transform coefficients of the individual bands.

The voltage under normal condition is almost pure

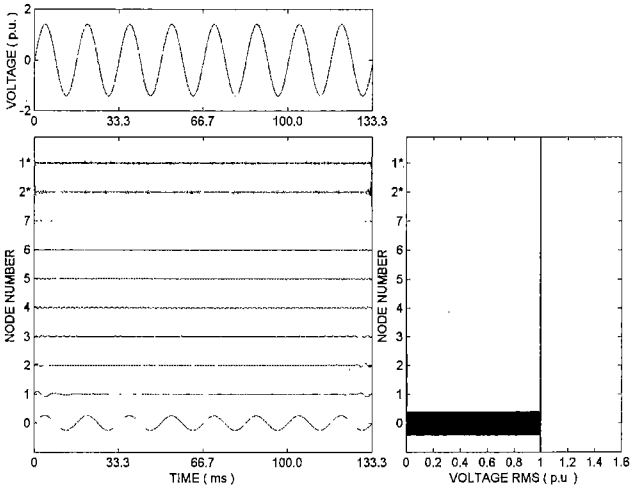

Fig. 3. Voltage during normal condition. Top panel is the original waveform, bottom right is the distribution panel, and bottom left is the time-frequency panel. The vertical line in the distribution panel indicates 1 p.u. rms value. (The ratio of node 0, nodes 1∼7, and nodes 1*∼2* in the time-frequency panel is 1:20:100.)

Table 2. Comparison results for normal voltage.

Node	FFT	BTWT
0	1.0000	1.0000
1	0.0053	0.0053
2	0.0026	0.0029
3	0.0020	0.0019
4	0.0014	0.0017
5	0.0014	0.0014
6	0.0011	0.0011
7	0.0010	0.0010
2*	0.0019	0.0019
1*	0.0018	0.0018
TOTAL	1.0000	1.0000
error(%)	-0.00001776	0.00000000
THBD(%)	0.7513	0.7390

sine wave of fundamental frequency as indicated by very small harmonic contents. The rms value of the fundamental frequency at node 0 is 1 p.u. Table 2 shows the rms values of each band of the proposed technique along with the results obtained from the FFT method. From the table, the rms values of each band of the proposed technique closely match the results of FFT method. The error indicates the difference in total rms value between each technique and the time domain reference. The total rms value of time domain reference is calculated analytically using (8). The proposed technique provides no error under the precision cited, meaning this wavelet technique produces the same total rms as the time domain method. However, the FFT method owns small error. The THBD values are also shown in the table and the values closely match to each other.

Harmonic Disturbance: The harmonic disturbance waveform is shown in Fig. 4. The harmonics can be easily seen mainly at nodes 1∼7 in the distribution panel. There are three significant harmonics detected

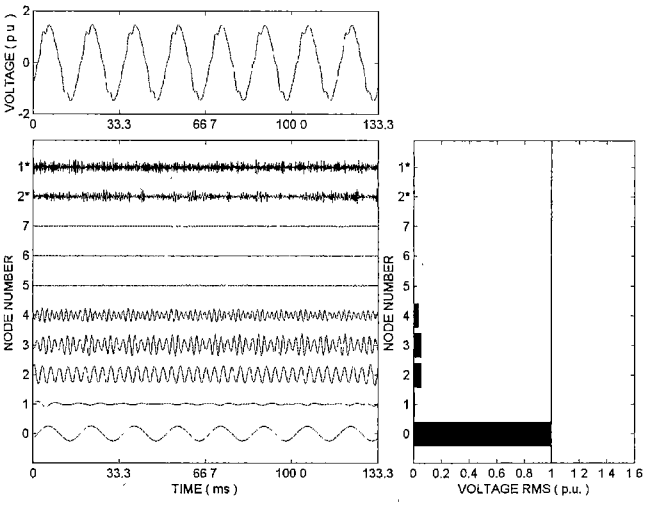

Fig. 4. Harmonic disturbance. (The ratio of node 0, nodes 1∼7, and nodes 1*∼2* in the time-frequency panel is 1:20:100.)

Table 3. Comparison results for harmonic disturbance.

Node	FFT	BTWT
0	1.0000	1.0000
1	0.0074	0.0074
2	0.0542	0.0545
3	0.0553	0.0552
4	0.0332	0.0332
5	0.0027	0.0027
6	0.0021	0.0021
7	0.0016	0.0015
2*	0.0039	0.0040
1*	0.0053	0.0053
TOTAL	1.0036	1.0036
error(%)	-0.00463523	0.00000000
THBD(%)	8.5289	8.4709

at nodes 2, 3, and 4, and these harmonics are stationary as seen from their waveforms on the time-frequency panel. There is no localization property observed at nodes 1* and 2* from the time-frequency panel. The quantity of rms of individual bands is shown in Table 3. The table shows that the rms values of each band closely match the FFT method results. The proposed technique provides no error in total rms value while the FFT method does. These prove that the quantification results using the proposed technique are accurate.

Flat-top Waveform: The flat-top waveform is shown in Fig. 5. This waveform, like the harmonic disturbance waveform, contains stationary harmonics as shown in the time-frequency panel. From the localization property observed at node 1*, one can see short silent intervals which coincide with the intervals of flat waveform at the voltage maxima and minima. Since the waveform is stationary, these silent intervals are periodic. There is small amount reduction in the rms value

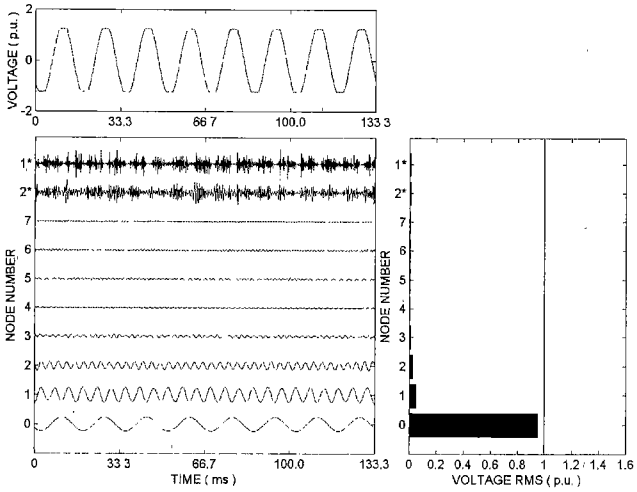

Fig. 5. Flat-top waveform. (The ratio of node 0, nodes 1∼7, and nodes 1*∼2* in the time-frequency panel is 1:20:100.)

Table 4. Comparison results for flat-top waveform.

Node	FFT	BTWT
0	0.9469	0.9469
1	0.0493	0.0493
2	0.0264	0.0263
3	0.0087	0.0088
4	0.0026	0.0025
5	0.0055	0.0055
6	0.0036	0.0037
7	0.0026	0.0023
2*	0.0067	0.0068
1*	0.0078	0.0078
TOTAL	0.9487	0.9487
error(%)	-0.00001228	0.00000000
THBD(%)	6.1156	6.1096

at the lowest band as seen in the distribution panel, and this is due to the cutting waveform at the voltage maxima and minima. Table 4 shows the rms values of each band, the total rms, the errors, and the THBD. The results confirm that the proposed technique is accurate.

5.2 **Non-Stationary Disturbances** These disturbance waveforms have time-varying amplitude during the observation period.

Voltage Sag: The sag waveform is shown in Fig. 6. The sag initiation and at voltage recovery are detected and localized at nodes 1* and 2*. The other nodes also show the same phenomena. However, only node 1* or node 2* is used to estimate the interval of the sag. This interval is achieved by taking the time of the peaks of waveform at either node 1* or node 2*. In this disturbance, we simply use the peaks at node 2*, and the interval is found to be about $T_1 = 68.36$ ms. Since the waveform is non-stationary, the harmonics in the time-frequency panel are also time-variant. The rms value during the observation period at the lowest band is significantly reduced as seen in the distribution panel. The voltage magnitude during the sag is calculated using (10) and it is about 0.7521 p.u., whereas if it is measured directly by tracking the sag waveform at the lowest band in the time-frequency panel the magnitude is 0.7616 p.u. The quantity of rms and THBD is shown in Table 5. The results in the table show that the proposed

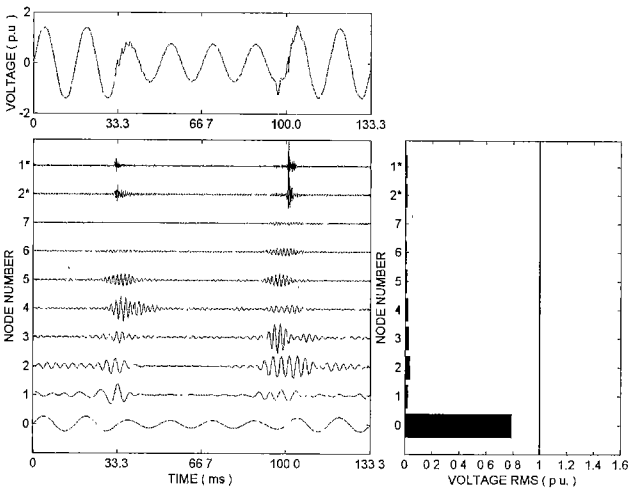

Fig. 6. Voltage sag. (The ratio of node 0 and the others in the time-frequency panel is 1:20.)

Table 5. Comparison results for voltage sag.

Node	FFT	BTWT
0	0.7909	0.7909
1	0.0234	0.0229
2	0.0318	0.0314
3	0.0236	0.0241
4	0.0220	0.0219
5	0.0143	0.0145
6	0.0069	0.0073
7	0.0034	0.0032
2*	0.0127	0.0123
1*	0.0143	0.0146
TOTAL	0.7929	0.7929
error(%)	-0.00069117	0.00000000
THBD(%)	7.1810	7.1482

technique provides almost the same values as the FFT method. Again, unlike the FFT method, this wavelet technique provides no error in total rms value.

Voltage Swell: The swell waveform is shown in Fig. 7. The swell is detected and localized at nodes 1* and 2*. The interval of the swell obtained from node 2* is about $T_1 = 63.66$ ms. Similar to the sag, the harmon-

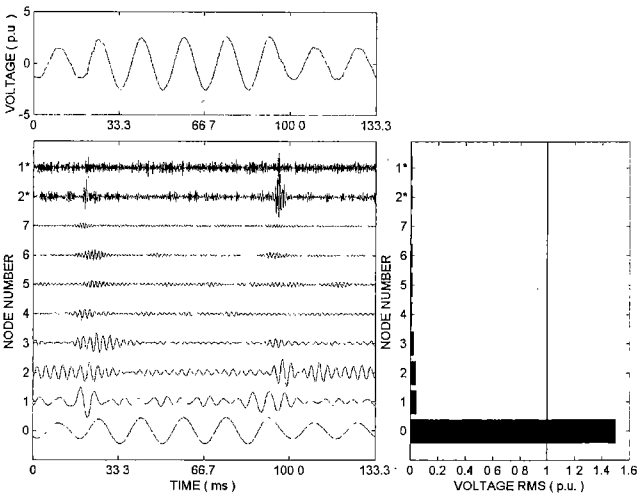

Fig. 7. Voltage swell. (The ratio of node 0, nodes 1∼7, and nodes 1*∼2* in the time-frequency panel is 1:20:60.)

Table 6. Comparison results for voltage swell.

Node	FFT	BTWT
0	1.4991	1.4988
1	0.0393	0.0399
2	0.0406	0.0396
3	0.0207	0.0206
4	0.0086	0.0100
5	0.0097	0.0105
6	0.0097	0.0097
7	0.0048	0.0049
2*	0.0073	0.0071
1*	0.0069	0.0070
TOTAL	1.5004	1.5001
error(%)	-0.01885879	0.00000000
THBD(%)	5.0496	4.2207

ics in the time-frequency panel are time-variant. The rms value during the observation period at the lowest band is largely increased as shown in the distribution panel. The calculated magnitude during the swell is about 2.5541 p.u., whereas if it is measured by tracking the lowest band waveform the magnitude is 2.5528 p.u. The rms value of the individual bands, the errors, and the THBD are quantified in Table 6. The table shows that the rms values of each band and the THBD values are almost the same as the FFT method results.

Momentary Interruption: The typical example of this disturbance is shown in Fig. 8. The start and end points of the interruption are clearly detected and localized at particularly nodes 1* and 2*. By taking the peaks of the waveform at node 1*, the interruption interval is about $T_1 = 69.79$ ms. The harmonics are time-varying amplitudes. The rms value at the lowest band is largely decreased as shown in the distribution panel. The calculated magnitude during the interruption is about 0.0549 p.u., and the result obtained by tracking the waveform at the lowest band is about 0.0497 p.u. The comparison of rms and THBD results in Table 7 shows no significant difference between this proposed technique and the FFT method.

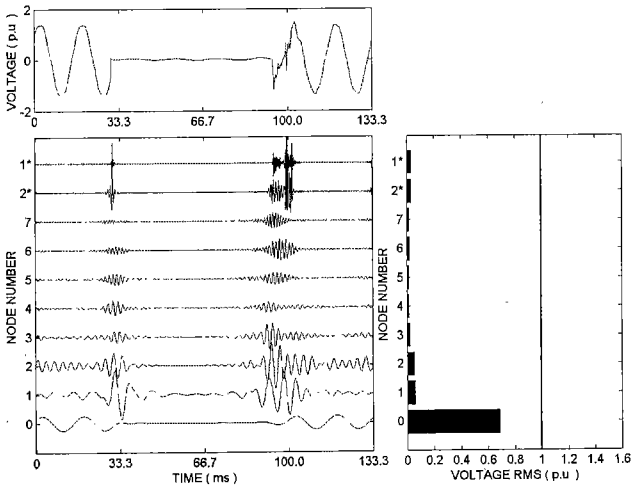

Fig. 8. Momentary interruption. (The ratio of node 0 and the others in the time-frequency panel is 1:20.)

Table 7. Comparison results for momentary interruption.

Node	FFT	BTWT
0	0.6857	0.6854
1	0.0600	0.0602
2	0.0457	0.0494
3	0.0242	0.0226
4	0.0146	0.0138
5	0.0121	0.0134
6	0.0174	0.0173
7	0.0144	0.0109
2*	0.0272	0.0277
1*	0.0295	0.0307
TOTAL	0.6920	0.6920
error(%)	-0.00691346	0.00000000
THBD(%)	13.6858	13.7640

6. Concluding Remarks

A simple yet powerful PQ monitoring technique based on modified binary-tree wavelet transform has been introduced and evaluated. The property of this wavelet analysis shows the ability of this technique to detect, classify, and accurately quantify different type of voltage disturbances. The evaluation is performed on stationary and non-stationary disturbances. The results of this proposed technique can be summarized as follows:
Stationary Disturbances: (1) The rms at the lowest band is nearly or equals to 1 p.u. in case of harmonic disturbance, and there is small amount reduction of that value in case of flat-top waveform. (2) The harmonics, particulary at nodes 1∼7, are time-invariant. (3) Another difference between harmonic and flat-top disturbances is the waveform signature at node 1*.
Non-Stationary Disturbances: (1) The large variation of rms value at the lowest band in the distribution panel allows to classify the type of non-stationary disturbances. This classification procedure combined with the voltage magnitude measurement can accurately discriminate mainly between sag and momentary interruption. (2) The harmonics occurred at nodes 1∼7 are time-variant. (3) The interval of disturbances is detected and localized at either node 1* or node 2*. (4) The localization properties at nodes 1* and 2* differ from the stationary cases.

Using the proposed technique, the quantification results of PQ indices confirm that (1) in all cases the rms values of each individual band and the THBD result closely match with those obtained from the FFT method, (2) in all cases the result of total rms is the same value as that obtained from the time domain method under the precision cited, and (3) the voltage magnitude measurement results are nearly the same as the tracking results of the disturbance waveform at the lowest band. Final remark, this wavelet technique combined with a pattern recognition method can be proposed to construct an automated recognition system.

(Manuscript received June 1, 2001, revised September 6, 2001)

References

(1) Santoso, S., E.J. Powers, W.M. Grady, and P. Hofmann, Power quality assesment via wavelet transform analysis, IEEE Trans. Power Delivery, 11, 924-930, 1996.
(2) Gaouda, A.M., M.M.A. Salama, M.R. Sultan, and A.Y.

Chikhani, Application of multiresolution signal decomposition for monitoring short-duration variations in distribution systems, IEEE Trans. Power Delivery, 15, 478-485, 2000.
(3) Angrisani, L., P. Daponte, M. D'Apuzzo, and A. Testa, A measurement method based on wavelet transform for power quality analysis, IEEE Trans. Power Delivery, 13, 990-998, 1998.
(4) Santoso, S., W.M. Grady, E.J. Powers, J. Lamoree, and S.C Bhatt, Characterization of distribution power quality events with fourier and wavelet transforms, IEEE Trans. Power Delivery, 15, 247-254, 2000.
(5) Karimi, M., H. Mokhtari, and M. R. Iravani, Wavelet based online disturbance detection for power quality applications, IEEE Trans. Power Delivery, 15, 1212-1220, 2000.
(6) Robertson, D.C, O.I. Camps, J.S. Mayer, and W.B. Gish, Wavelets and electromagnetic power system transients, IEEE Trans. Power Delivery, 11, 1050-1058, 1996.
(7) Huang, S.J., C.T.Hsieh, and C.L. Huang, Application of Morlet wavelet to supervise power system disturbances, IEEE Trans. Power Delivery, 14, 235-241, 1999.
(8) Pandey, S.K., and L. Satish, Multiresolution signal decomposition: a new tool for fault detection in power transformers during impulse tests , IEEE Trans. Power Delivery, 13, 1194-1200, 1998.
(9) YuHua, G., and M.H.J. Bollen, Time-frequency and time-scale domain analysis of voltage disturbances, IEEE Trans. Power Delivery, 15, 1279-1284, 2000.
(10) Poisson, O., P. Rioual, and M. Meunier, Detection and measurement of power quality disturbances using wavelet transform, IEEE Trans. Power Delivery, 15, 1039-1044, 2000.
(11) Yoon, W.K., and M.J. Devaney, Power measurement using the wavelet transform, IEEE Trans. Instrum. Meas., 47, 1205-1209, 1998.
(12) Wickerhauser, M.V., Adapted wavelet analysis from theory to software, IEEE Press, New York, USA, 237-298, 1994.
(13) Rioul, O., and M. Vetterli, Wavelets and signal processing, IEEE Signal Processing Magazine, 14-38, October 1996.
(14) Beylkin, G., Wavelet, Multiresolution analysis and fast numerical algoritms, in INRIA lectures, 1-36, 1994.

Appendix

Calculation of Disturbance Magnitude

Consider a voltage sag below. The total observation period is T and the duration of disturbance is T_1, and assume that the nominal voltage rms of fundamental frequency f_0 during normal condition (no disturbance) is 1 p.u. Now, the voltage rms V_0 during period T is

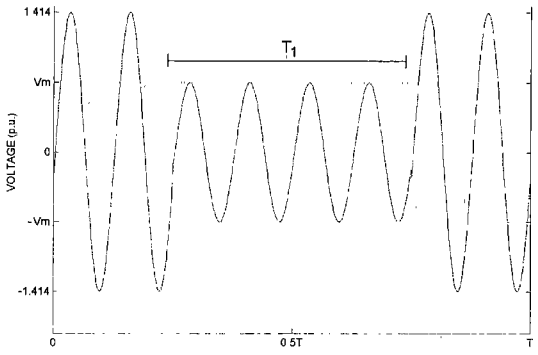

app. Fig. 1. Voltage sag of fundamental cycle.

$$V_0 = \sqrt{\frac{1}{T}\left[\int_0^{T-T_1} (\sqrt{2}\sin\omega t)^2\ dt + \int_0^{T_1} (V_m \sin\omega t)^2\ dt\right]}\ \text{p.u.}, \tag{A1}$$

where $\omega = 2\pi f_0$, and V_m is the voltage magnitude of disturbance to be solved. Arranging (A1) then

$$V_0^2 T = 2\int_0^{T-T_1} \sin^2\omega t\ dt + V_m^2 \int_0^{T_1} \sin^2\omega t\ dt, \tag{A2}$$

and it is known that $\int_0^x \sin^2\omega t\ dt = 0.5x + \frac{0.25}{\omega}\sin 2\omega x$. Hence, (A2) becomes

$$V_0^2 T = T - T_1 + \frac{0.5}{\omega}\sin 2\omega(T-T_1) + V_m^2\left(0.5T_1 + \frac{0.25}{\omega}\sin 2\omega T_1\right), \tag{A3}$$

and, by arranging (A3), finally the magnitude during disturbance is

$$V_m = \sqrt{\frac{V_0^2 T\omega - \omega(T-T_1) - 0.5\sin 2\omega(T-T_1)}{0.5\omega T_1 + 0.25\sin 2\omega T_1}}\ \text{p.u.} \tag{A4}$$

If one is interested in rms value, the V_m is divided by a factor of $\sqrt{2}$. Formula (A4) is also used to quantify the magnitude of swell and momentary interruption.

Effrina Yanti Hamid (Non-member) She was born in Indonesia in 1972. She received the bachelor and master degrees in electrical engineering from Institut Teknologi Bandung, Indonesia in 1995 and 1998, respectively. Now, she is a doctor course student in the Department of Electrical Engineering, Osaka University. Her main interest is in signal processing and its application to power system.

Zen-Ichiro Kawasaki (Member) He was born in Japan in 1949. He received the B.S., M.S. and Dr. Eng. degrees in communication engineering from Osaka University, Japan in 1973, 1975 and 1978, respectively. In 1989, he joined the Department of Electrical Engineering, Osaka University. Currently, he is a professor at the Department of Communication Engineering in the same university. His current research interests are in diagnosis techniques of power apparatus and the electromagnetic of lightning discharges. Dr. Zen-Ichiro Kawasaki is a member of IEEE, IEE of Japan, American Geophysical Union (AGU), and The Society of Atmospheric Electricity of Japan (SAEJ).

Hirotaka Yoshida (Member) He received M.S. degree in electrical engineering in 1976 from Doshisha University, Kyoto, Japan. He has been working at The Kansai Electric Power Company from 1976. His research interests include analysis, planning, and operation of power systems. He is a member of IEE of Japan.

Hirosuke Doi (Member) He graduated an electric course of Technical High School in Japan, in 1965. He had joined The Kansai Electric Power Company, Japan. He has been working at Kansai Electric Instrument Company. He was commended to the persons of scientific and technological research merits by the Minister of State for Science anf Technology in 1991. He was awarded for the Technical Advancement from IEE in 1991. He is a member of IEE of Japan.